

77 K as arising from the dipole allowed  $E_u$  spin-orbit component of the  ${}^3A_{2u}$  term ( $D_{4h}$  symmetry). This leads us to assign the shorter lived higher energy emitting level as an  $E_u$  state (thus doubly degenerate) and the lower energy emitting level as the forbidden  $A_{1u}$  spin-orbit component derived from the  ${}^3A_{2u}$  term. In the case of the bis(arphos) complexes (cis isomer,  $C_{2v}$ ; trans isomer,  $D_{2h}$ ) and cod complexes ( $C_{2v}$ ), the lowering of symmetry splits the degenerate  $E_u$  level into two dipole-allowed components in the lower symmetry groups. In the temperature vs. lifetime data and also the spectral data, we see no evidence for the splitting of the  $E_u$  level in these complexes. Apparently the levels are accidentally degenerate or separated by only a few wavenumbers.

Trends in the data presented in Table III allow us to draw a number of conclusions concerning the nature of the lowest emitting term of these complexes. Most apparent is the larger  $\Delta\epsilon$  values and lesser  $\tau$  values of the Ir(I) species compared to those of Rh(I). These values reflect the greater spin-orbit coupling constant of Ir(I); this is also manifested in the larger extinction coefficients of the triplet absorption bands of all the Ir(I) complexes. We also ascribe the increase in  $\Delta\epsilon$  as arsenic is substituted for phosphorus to the larger spin-orbit coupling constant of the former atom. This dependence of  $\Delta\epsilon$  on the nature of the chelated atom clearly demonstrates the involvement of these atoms in the excited triplet. One expects the aromatic linkage between phosphorous atoms in the dpbe ligand to delocalize some of the charge density off the phosphorus atoms; a correspondingly slightly reduced  $\Delta\epsilon$  value [ $\zeta(\text{phosphorus}) \gg \zeta(\text{carbon})$ ] is found. Conversely, the replacement of the phenyl rings in diphos with cyclohexyl groups in the dcpe ligand should keep the charge density on the phosphorus atoms;  $\Delta\epsilon$  also increases. Conclusions drawn from trends in the  $\tau$  values are risky since these parameters are

related to the radiative lifetimes by the quantum yields, which we do not know. The only  $\tau$  value that stands out is the relatively short  $\tau_1$  value for  $[\text{Ir}(\text{2=phos})(\text{cod})]\text{PF}_6$ . Perhaps the replacement of a phosphine with cod facilitates geometrical distortions that reduce the forbiddenness of the lower level.

We have established the existence of a two-level emitting manifold in these complexes from analysis of the lifetimes vs. temperature and from spectral band-shape data. The substantial reduction of the molar extinction coefficients upon replacement of a diphosphine with cod and the effect on  $\Delta\epsilon$  upon replacing P with As in the ligands demonstrate a charge-transfer component in the low-energy states. This component appears to be predominantly localized on the P or As atom. Although not yet quantified, the metal-localized component of the low-energy excited states is demonstrated by the relative insensitivity of the spectral features to changes in ligands, particularly replacement of phosphorus with arsenic, and the absence of measurable splitting of degenerate levels upon reducing the core symmetry. The  $2500\text{-cm}^{-1}$  red shift of all the spectral features upon replacement of a diphosphine with cod is attributed to destabilization of the d orbitals due to closer approach of the diphosphine to the metal center.

**Acknowledgments.** Research was supported by the Directorate of Chemical Sciences, Air Force Office of Scientific Research, Grant AFOSR-80-0038. We thank Matthey-Bishop for a generous loan of rhodium and iridium chlorides.

**Registry No.**  $[\text{Rh}(\text{2=phos})_2]\text{ClO}_4$ , 57749-19-6;  $[\text{Rh}(\text{dpbe})_2]\text{ClO}_4$ , 80340-14-3;  $[\text{Rh}(\text{dpp})_2]\text{PF}_6$ , 80340-15-4;  $[\text{Rh}(\text{dcpe})_2]\text{PF}_6$ , 80340-17-6;  $[\text{Rh}(\text{arphos})_2]\text{PF}_6$ , 80340-18-7;  $[\text{Rh}(\text{2=ars})_2]\text{PF}_6$ , 60646-26-6;  $[\text{Rh}(\text{2=phos})(\text{cod})]\text{PF}_6$ , 80340-19-8;  $[\text{Ir}(\text{diphos})_2]\text{ClO}_4$ , 15685-14-0;  $[\text{Ir}(\text{2=phos})_2]\text{ClO}_4$ , 36390-40-6;  $[\text{Ir}(\text{dpbe})_2]\text{ClO}_4$ , 80340-21-2;  $[\text{Ir}(\text{arphos})_2]\text{PF}_6$ , 80375-21-9;  $[\text{Ir}(\text{diphos})(\text{cod})]\text{PF}_6$ , 61817-48-9;  $[\text{Ir}(\text{2=phos})(\text{cod})]\text{PF}_6$ , 80340-22-3;  $[\text{Ir}(\text{dpbe})(\text{cod})]\text{PF}_6$ , 80340-24-5.

Contribution from the Istituto di Teoria e Struttura Elettronica e Comportamento Spettrochimico dei Composti di Coordinazione del CNR, Area della Ricerca di Roma, Monterotondo Stazione, Roma, Italy

## EPR Spectra of Eight-Coordinated Complexes of the Early Transition Metals with Sulfur and Selenium Donor Ligands. 3.<sup>1,2</sup> Vanadium(IV) and Niobium(IV) Dithio- and Diselenocarbamates

D. ATTANASIO,\* C. BELLITTO,\* A. FLAMINI,\* and G. PENNESI

Received September 1, 1981

Single-crystal and powder EPR studies of the eight-coordinated complexes tetrakis(*N,N*-diethyldithiocarbamato)vanadium(IV), tetrakis(*N,N*-diethyldithiocarbamato)niobium(IV), and tetrakis(*N,N*-diethyldiselenocarbamato)vanadium(IV), diluted in the diamagnetic Ti(IV) analogues, are reported. Two, chemically inequivalent, crystallographic sites are present in the unit cell of the two isomorphous host compounds. They are differently populated by the paramagnetic ions, the most asymmetric site accounting for about 75% of the total V(IV) or Nb(IV) concentration. All the different EPR signals arise from discrete eight-coordinated species, with a molecular geometry close to the ideal triangular dodecahedron ( $D_{2d}$ ). The mixing coefficients in a ground-state orbital of the type  $a|x^2 - y^2\rangle - b|z^2\rangle$  have been obtained from the experimental results and related to the deviation from pure  $D_{2d}$  symmetry. However, no simple relationship could be found between this distortion and the type of ligands or metal ion involved. Low-intensity satellite lines have been observed in the spectrum of  $\text{V}/\text{Ti}(\text{Et}_2\text{dsec})_4$  and attributed to the hyperfine coupling of the unpaired electron with four different selenium nuclei. No splitting from the other four selenium ligands could be observed. This result has been related to the inequivalence of the A and B ligand sites of the dodecahedron and, specifically, to the different overlap between the metal ion ground-state orbital and the ligand  $\pi_{\perp}$  orbitals.

### Introduction

As a continuation of our interest in eight-coordinated complexes of sulfur and selenium donor ligands, we report here a single-crystal and powder EPR study of tetrakis(*N,N*-di-

ethyldithiocarbamato)vanadium(IV),  $\text{V}(\text{Et}_2\text{dtc})_4$ , tetrakis(*N,N*-diethyldithiocarbamato)niobium(IV),  $\text{Nb}(\text{Et}_2\text{dtc})_4$ , and tetrakis(*N,N*-diethyldiselenocarbamato)vanadium(IV),  $\text{V}(\text{Et}_2\text{dsec})_4$ , substitutionally diluted in the diamagnetic Ti(IV) analogues.

In a previous EPR work on eight-coordinated dithiocarbonylato complexes,<sup>1,2</sup> with the same metal ions, we have shown that these compounds have an essentially  $|x^2 - y^2\rangle$

(1) Attanasio, D.; Bellitto, C.; Flamini, A. *Inorg. Chem.* 1980, 19, 3419.  
(2) Attanasio, D.; Bellitto, C.; Flamini, A.; Pennesi, G. *Chem. Phys. Lett.* 1980, 72, 307.

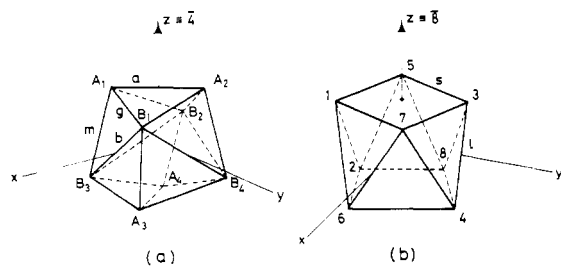


**Figure 1.** The  $D_{2d}$  triangular dodecahedron (a) and the  $D_{4d}$  square antiprism (b). The molecular axis systems used throughout the text are indicated. Ligand sites and polyhedral edges are labeled according to Hoard and Silverton.<sup>25</sup>

ground-state orbital with a small admixture of  $|z^2\rangle$ . This corresponds to a basically  $D_{2d}$  dodecahedral geometry (Dod, Figure 1a), with a superimposed small distortion toward the  $D_{4d}$  square antiprism (SAP Figure 1b).

The two ideal polyhedra differ slightly in energy and correspond to the two minima found in the potential energy surfaces calculated by Blight and Kepert.<sup>3,4</sup> The degree of distortion and other details of the observed geometries have been ascribed, by some authors, to smaller energy terms such as the  $\pi$ -bonding ability of the ligand or the electronic structure of the metal ion.<sup>5-7</sup>

However, the isolation of a new crystal form of tetrakis(dithioacetato)molybdenum(IV),  $\text{Mo}(\text{dta})_4$ , and the analysis of its V(IV)-doped crystals,<sup>1</sup> have shown that these smaller effects can be completely "swamped" by solid-state packing forces, making difficult the experimental evaluation of their relevance.

We have now extended the work to the analogous dithio- and diselenocarbamate complexes. The main purpose was to extend the correlation between structure and electronic properties of eight-coordinated complexes by varying the ligands and the molecular symmetry of the host compounds. From this point of view  $\text{Ti}(\text{Et}_2\text{dtc})_4$  and  $\text{Ti}(\text{Et}_2\text{dsec})_4$ , which contain geometrically different molecules in the unit cell, were particularly suitable matrixes.

The diselenocarbamate complexes were prepared to obtain a more detailed picture of the bonding from the possible observation of ligand hyperfine structure. So far this piece of information has been reported only for the isotropic spectrum of the dodecahedral ion  $[\text{Mo}(\text{CN})_8]^{3-}$ .<sup>8,9</sup> Unfortunately  $\text{Nb}(\text{Et}_2\text{dsec})_4$  proved to be too unstable, even in the dilute state, and only the much more stable vanadium complex could be measured.

## Experimental Section

**Reagents.** All manipulations were carried out under dry, oxygen-free nitrogen. Dried and freshly distilled solvents were used and degassed immediately before use.  $(\text{C}_2\text{H}_5)_2\text{CS}_2\text{Na}^+$ , diethyldithiocarbamic acid sodium salt ( $\text{Na}(\text{Et}_2\text{dtc})$ ), was obtained commercially and dried under vacuum at 80 °C.  $(\text{C}_2\text{H}_5)_2\text{CSe}_2\text{H}$ , diethyldiselenocarbamic acid ( $\text{Et}_2\text{dsecH}$ ), was prepared according to Barnard and Woodbridge<sup>10</sup> and used as its diethylammonium salt. Commercial  $\text{NbCl}_5$  was purified before use by vacuum sublimation at 100 °C. Commercial  $\text{TiCl}_4$  was used after distillation at atmospheric pressure.

**Preparation of Complexes.**  $\text{Nb}(\text{Et}_2\text{dtc})_4$ ,<sup>11</sup>  $\text{Ti}(\text{Et}_2\text{dtc})_4$ ,<sup>11</sup> and  $\text{Ti}(\text{Et}_2\text{dsec})_4$  were all obtained by similar methods. The last complex

**Table I.** Molecular Geometry of Tetrakis(diethyldithiocarbamato)titanium(IV)

	molecule 1	molecule 2	ref
$\Delta(\text{Dod}), \text{Å}^a$	0.044	0.039	15
$\Delta(\text{SAP}), \text{Å}^a$	0.181	0.158	15
$\delta, \text{deg}^{a,b}$	28.4, 39.0, 30.6, 39.9	27.6, 31.6, 40.6, 41.0	15
M-S <sub>A</sub> , Å	2.62	2.60	14
M-S <sub>B</sub> , Å	2.51	2.53	14
$\theta_A, \text{deg}^a$	35.4	34.8	14
$\theta_B, \text{deg}^a$	77.0	78.0	14

<sup>a</sup> Minimum root-mean-square difference between the actual coordinates and those of the ideal polyhedra. The  $\delta$  angles are the dihedral angles among pairs of triangular faces of the Dod.  $\theta_A$  and  $\theta_B$  are the angles between the 4 axis and M-A or M-B directions. See ref 15. <sup>b</sup> The values required for the two ideal polyhedra, from the "so-called" hard-sphere model (HSM) are  $29.5 \times 4$  (Dod) or  $0.0 \times 2$  and  $52.4 \times 2$  (SAP). Symmetry requires only four identical values or two zero and two equal values, respectively.

has not been reported before and therefore details of this preparation are given below.

$\text{Ti}(\text{Et}_2\text{dsec})_4$ . The ligand (6.3 g,  $1.99 \times 10^{-2}$  mol) was dissolved in 100 mL of toluene.  $\text{TiCl}_4$  (0.756 g,  $0.438 \text{ mL}$ ,  $3.995 \times 10^{-3}$  mmol) was added dropwise to the solution and stirring was continued overnight. The solution was heated at 60 °C, filtered, and reduced in volume. On cooling a brick-red solid was obtained. The product was washed with acetonitrile and petroleum ether and then dried under vacuum. Anal. Calcd for  $\text{C}_{20}\text{H}_{20}\text{N}_4\text{Se}_8\text{Ti}$ : C, 23.64; H, 3.97; N, 5.51; Se, 62.16; Ti, 4.71. Found: C, 23.64; H, 3.92; N, 5.41; Se, 62.13; Ti, 4.66.

$\text{V}(\text{Et}_2\text{dtc})_4$ <sup>11</sup> and  $\text{V}(\text{Et}_2\text{dsec})_4$  were prepared by direct reaction of the appropriate ligand with vanadyl sulfate in acetonitrile. It is known<sup>12</sup> that this procedure, in the case of the  $\text{Et}_2\text{dtc}$  ligand, gives the  $\text{VO}^{2+}$  derivative. However, small quantities of the  $\text{V}^{4+}$  compound must be present since the crude product we used substitutes  $\text{Ti}^{4+}$  in the diamagnetic host. In the case of the seleno derivative we found that the crude product was mainly the  $\text{V}^{4+}$  compound.

**Tantalum(IV) Complexes.** Several attempts were made to prepare analogous Ta(IV) compounds.  $\text{TaCl}_5$  and  $\text{TaCl}_4 \cdot 2\text{py}$  were used as starting materials to obtain pure or magnetically diluted Ta(IV) species directly from the preparation. Although some of the samples displayed more or less intense EPR signals, we were not able to isolate pure compounds.

**Preparation of Doped Samples.** Microcrystalline powders of  $\text{V}/\text{Ti}(\text{Et}_2\text{dtc})_4$ ,  $\text{Nb}/\text{Ti}(\text{Et}_2\text{dtc})_4$ , and  $\text{V}/\text{Ti}(\text{Et}_2\text{dsec})_4$  were obtained by dissolving in  $\text{CS}_2$  the corresponding complexes in the appropriate percentage. After filtration and subsequent addition of petroleum ether, the solutions, stored at 3 °C overnight, afforded red-brown crystals. When the ratio of  $\text{CS}_2$  to petroleum ether was varied, a crystal suitable for single-crystal measurements could be obtained. The best doping concentrations were found by trial and error.

Due to different solubilities large concentrations (up to 10%) of the paramagnetic ions had to be used, in some cases, to obtain measurable EPR signals. However, the actual concentration in the crystals was probably much lower since line broadening effects could not be detected.

**Physical Measurements.** Room-temperature EPR spectra were recorded at X- or Q-band frequency with a Varian E-9 spectrometer. Details of the experimental technique and of the computer programs used to analyze the single-crystal spectra have been reported elsewhere.<sup>1</sup> Rotational data were recorded in an orthogonal coordinate system,  $x, y, z$ , related to the crystal axis system by an Euler transformation ( $x$  and  $a$  coincide). Crystals of  $\text{Nb}/\text{Ti}(\text{Et}_2\text{dtc})_4$  and  $\text{V}/\text{Ti}(\text{Et}_2\text{dsec})_4$  were oriented with oscillation and zero-layer Weissenberg photographs, taken with  $\text{Cu K}\alpha$  radiation.

**Crystal Structures.** Of all the compounds investigated in this paper,  $\text{Ti}(\text{Et}_2\text{dtc})_4$  is the only one for which complete structural information is available.<sup>13,14</sup> The complex crystallizes in the triclinic space group

(3) Blight, D. G.; Kepert, D. L. *Theor. Chim. Acta* **1968**, *11*, 51.

(4) Blight, D. G.; Kepert, D. L. *Inorg. Chem.* **1972**, *11*, 1556.

(5) Hyde, J.; Zubietta, J. *J. Inorg. Nucl. Chem.* **1977**, *39*, 289.

(6) Steffen, W. L.; Fay, R. C. *Inorg. Chem.* **1978**, *17*, 2120.

(7) Burdett, J. K.; Hoffmann, R.; Fay, R. C. *Inorg. Chem.* **1978**, *17*, 2553.

(8) Weissman, S. I.; Cohn, M. *J. Chem. Phys.* **1957**, *27*, 1440.

(9) McGarvey, B. R. *Inorg. Chem.* **1966**, *5*, 476.

(10) Barnard, D.; Woodbridge, D. T. *J. Chem. Soc.* **1961**, 2922.

(11) Bradley, D. C.; Gitlitz, M. H. *J. Chem. Soc. A* **1969**, 1152.

(12) Bereman, R. D.; Nalewajek, D. *J. Inorg. Nucl. Chem.* **1978**, *40*, 1309.

(13) Colapietro, M.; Vaciego, A.; Bradley, D. C.; Hursthouse, M. B.; Rendall, I. V. *J. Chem. Soc., Chem. Commun.* **1970**, 743.

(14) Colapietro, M.; Vaciego, A.; Bradley, D. C.; Hursthouse, M. B.; Rendall, I. V. *J. Chem. Soc., Dalton Trans.* **1972**, 1052.

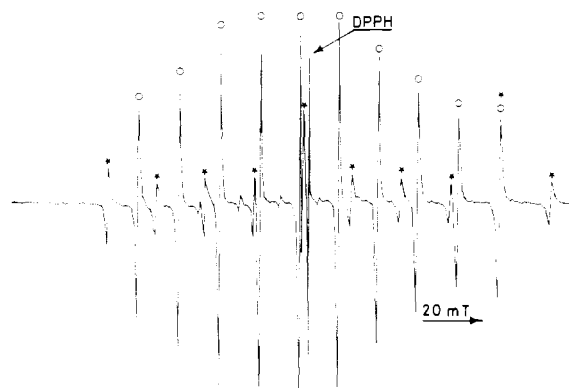


**Figure 2.** X-Band EPR spectrum of single crystal of Nb/Ti(Et<sub>2</sub>dtc)<sub>4</sub> at 300 K, for a general orientation of  $B_0$ . Lines from A (O) and B (\*) sites are indicated.

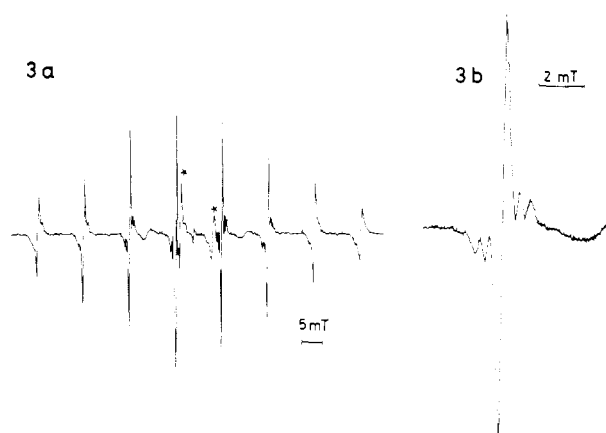


**Figure 3.** X-Band EPR spectrum of a single crystal of V/Ti(Et<sub>2</sub>dsec)<sub>4</sub> at 300 K, for a general orientation of  $B_0$ . Spectrum b is a magnification of the  $M_1 = +3/2$  line in spectrum a. The presence of two pairs of <sup>77</sup>Se satellites is evident. In this case the four selenium splittings are two by two equivalent. The origin of the two starred lines is not clear.

$P1$ , with  $Z = 4$ ,  $a = 11.435 \text{ \AA}$ ,  $b = 18.408 \text{ \AA}$ ,  $c = 15.382 \text{ \AA}$ ,  $\alpha = 96.39^\circ$ ,  $\beta = 91.62^\circ$ , and  $\gamma = 95.08^\circ$ . The unit cell contains two symmetry unrelated, slightly different molecules, which both approximate a dodecahedral geometry (subclass  $D_{2d}$ ,  $mmmm$ ). Some relevant crystallographic data, reported in Table I, indicate that molecule 2 is distorted along the interconnecting path between Dod and SAP, with a  $D_2$  point symmetry, whereas molecule 1 exhibits a small, but rather unusual distortion, which lowers its point symmetry below  $D_2$ .<sup>15</sup>

Ti(Et<sub>2</sub>dtc)<sub>4</sub>, Ti(Et<sub>2</sub>dsec)<sub>4</sub>, and their Nb- and V-doped powders all give rise to identical X-ray powder patterns. This means that the paramagnetic complexes of unknown structure enter the two isomorphous hosts without any appreciable crystal distortion. Furthermore, EPR results will show that the molecular geometries of Ti(Et<sub>2</sub>dtc)<sub>4</sub> and Ti(Et<sub>2</sub>dsec)<sub>4</sub>, as probed by V(IV) and Nb(IV), are almost identical.

Orientation of the magnetic axes in V/Ti(Et<sub>2</sub>dsec)<sub>4</sub> has been derived by use of crystallographic data from Ti(Et<sub>2</sub>dtc)<sub>4</sub>.

### Results

Representative single-crystal spectra of the systems Nb/Ti(Et<sub>2</sub>dtc)<sub>4</sub> and V/Ti(Et<sub>2</sub>dsec)<sub>4</sub> are reported in Figures 2–4. Two sets of eight (<sup>51</sup>V; 100%,  $I = 7/2$ ) or ten (<sup>93</sup>Nb; 100%,  $I = 9/2$ ) main lines are present in each spectrum, with an intensity ratio of about 3:1. In agreement with X-ray crystallographic data, the two sets never coincide. They correspond to the two symmetry unrelated, and hence magnetically and chemically inequivalent crystallographic sites. The spin-Hamiltonian parameters suggest that the paramagnetic ions

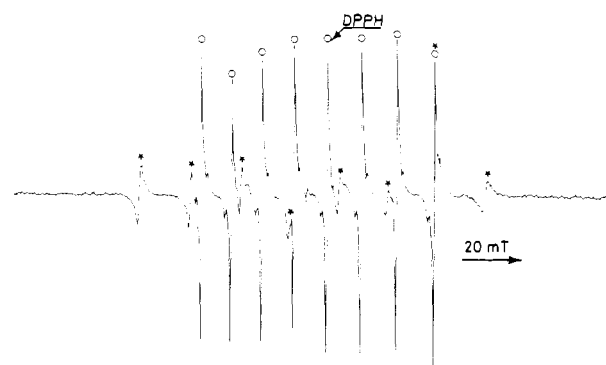


**Figure 4.** X-Band EPR spectrum of a single crystal of V/Ti(Et<sub>2</sub>dsec)<sub>4</sub> at 300 K, for a general orientation of  $B_0$ . Lines from A (O) and B (\*) sites are indicated. Partially resolved <sup>77</sup>Se lines are present.

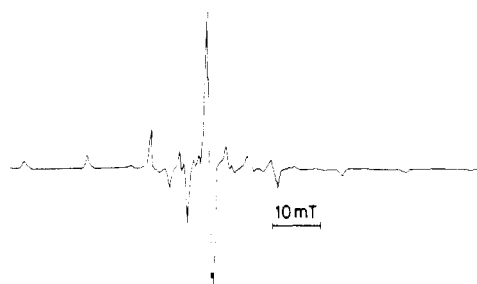


**Figure 5.** X-Band EPR powder spectrum of V/Ti(Et<sub>2</sub>dtc)<sub>4</sub> at 300 K.

**Table II.** X-Band Spin-Hamiltonian Parameters of V/Ti(Et<sub>2</sub>dsec)<sub>4</sub> and V/Ti(Et<sub>2</sub>dtc)<sub>4</sub> at 300 K<sup>a</sup>

principal axes	V/Ti(Et <sub>2</sub> dtc) <sub>4</sub> , <sup>b</sup> site A	V/Ti(Et <sub>2</sub> dsec) <sub>4</sub> , site A	V/Ti(Et <sub>2</sub> dsec) <sub>4</sub> , site B
$g_1$	1.989	2.0024	1.9948
$g_2$	1.981	1.9940	1.9934
$g_3$	1.956	1.9870	1.9904
$g_{av}$	1.975	1.9945	1.9924
$g_{iso}$	1.975 <sup>c</sup>		
$A_1$	120.8	114.3	110.4
$A_2$	51.2	53.9	46.6
$A_3$	27.7	31.2	42.0
$A_{av}$	66.6	66.5	66.3
$A_{iso}$	66.9 <sup>c</sup>		

<sup>a</sup> Hyperfine splittings are in units of  $10^{-4} \text{ cm}^{-1}$ . Their signs are discussed in the text. <sup>b</sup> Powder spectrum. <sup>c</sup> Reference 16.

**Table III.** Spin-Hamiltonian Parameters of Nb/Ti(Et<sub>2</sub>dtc)<sub>4</sub> at 300 K and Nb(Et<sub>2</sub>dtc)<sub>4</sub> at 300 and 110 K<sup>a</sup>

principal axes	Nb/ Ti(Et <sub>2</sub> dtc) <sub>4</sub> , site A <sup>d</sup>	Nb/ Ti(Et <sub>2</sub> dtc) <sub>4</sub> , site A <sup>e</sup>	Nb/ Ti(Et <sub>2</sub> dtc) <sub>4</sub> , site B <sup>d</sup>	Nb(Et <sub>2</sub> dtc) <sub>4</sub> <sup>c</sup>
$g_1$	1.9731	1.9732	1.9641	1.969
$g_2$	1.9511	1.9519	1.9583	1.962
$g_3$	1.9267	1.9275	1.9385	1.935
$g_{av}$	1.9503	1.9509	1.9536	1.955
$g_{iso}$				1.961
$A_1$	184.5	183.0	168.8	187
$A_2$	103.3	102.5	91.0	104
$A_3$	69.3	70.0	84.8	71
$A_{av}$	119.0	118.5	114.9	120.7
$A_{iso}$				116

<sup>a</sup> Hyperfine splittings are in units of  $10^{-4} \text{ cm}^{-1}$ ; their signs are discussed in the text. <sup>b</sup> Reference 2. <sup>c</sup> From liquid and frozen-resolution spectra in CS<sub>2</sub>. <sup>d</sup> X band. <sup>e</sup> Q band.

enter preferentially the most asymmetric sites (sites A).

The principal values of the tensors are listed in Tables II and III, respectively, for the V and Nb complexes. The experimental errors for the B sites are much larger than those

Table IV.  $^{77}\text{Se}$  Hyperfine Tensors in  $\text{V}/\text{Ti}(\text{Et}_2\text{dsec})_4^a$ 

	$A_1$	$A_2$	$A_3$	$A_{\text{av}}$
$^{77}\text{Se}_1$	18.1	16.0	8.8	14.3
$^{77}\text{Se}_2$	20.3	14.4	8.6	14.4
$^{77}\text{Se}_3$	18.7	14.3	9.2	14.1

<sup>a</sup> Given in units of  $10^{-4} \text{ cm}^{-1}$ .

for the A sites, due to the lower line intensity, combined with a stronger line-width anisotropy. Typical accuracies for the  $g$  and  $A$  values are 0.0002 and  $2.0 \times 10^{-5} \text{ cm}^{-1}$  (A sites) or 0.0010 and  $1.0 \times 10^{-4} \text{ cm}^{-1}$  (B sites).

In the case of  $\text{V}/\text{Ti}(\text{Et}_2\text{dte})_4$ , for which only powder spectra were measured (Figure 5), the two sites A and B could not be resolved, even at higher microwave frequencies (35 GHz). Comparison with the single-crystal results indicate that the experimental parameters belong to A-type vanadium ions. This is in agreement with the tendency, shown by the paramagnetic ions, to populate preferentially the most asymmetric site of the titanium matrix.

The spin-Hamiltonian parameters of pure  $\text{V}(\text{Et}_2\text{dte})_4^{16}$  and  $\text{Nb}(\text{Et}_2\text{dte})_4$ , derived from fluid and frozen-solution spectra, suggest that they are close in symmetry to the A site of  $\text{Ti}(\text{Et}_2\text{dte})_4$ . Solution data and previous results<sup>1</sup> indicate that all the metal hyperfine principal values are negative. Their principal directions were found, in all cases, to lie along the pseudododecahedral symmetry axes.  $A_1$  always coincides with the  $\bar{4}$  axis and has been assigned as  $A_2$ . The  $g$  tensor of  $\text{Nb}/\text{Ti}(\text{Et}_2\text{dte})_4$  has the same axis system:  $g_1$ ,  $g_2$ , and  $g_3$  being associated, respectively, with  $A^{\text{Nb}}_3$ ,  $A^{\text{Nb}}_2$ , and  $A^{\text{Nb}}_1$ . The largest misalignments are 3 and  $10^\circ$ , respectively, for sites B and A.

In the case of  $\text{V}/\text{Ti}(\text{Et}_2\text{dsec})_4$ , site A, the two axis systems are again almost coincident. However, the situation is unique in that the lowest  $g$  value,  $g_3$ , lies almost perpendicular to the  $\bar{4}$  direction, rather than parallel to it, as found in all the eight-coordinated complexes investigated so far.<sup>1</sup> As a result,  $g_1$ ,  $g_2$ , and  $g_3$  are associated, respectively, with  $A^{\text{V}}_3$ ,  $A^{\text{V}}_1$ , and  $A^{\text{V}}_2$ . The  $g$  and hyperfine principal directions of  $\text{V}/\text{Ti}(\text{Et}_2\text{dsec})_4$ , site B, are largely noncoincident. However, due to rather large experimental errors and to a very small  $g$  anisotropy, the above result is, probably, unreliable. Finally the magnetic sites A and B were associated, respectively, with the crystallographic molecules 1 and 2. This result was achieved by comparing the direction cosines that the  $\bar{4}$  direction and  $A_1$ , in the two sites, form with the crystal axis system.

Besides the main signals discussed so far, the spectra of  $\text{V}/\text{Ti}(\text{Et}_2\text{dsec})_4$ , A site, exhibit smaller lines, flanking each main peak, which vary from two to six in number, depending on the crystal orientation (Figure 4b). Measurements carried out at X- and Q-band frequencies showed the position and the intensity of these lines to be strictly field independent, thus confirming that they arise from a "true" hyperfine interaction with nuclear spins  $I = 1/2$ . By a least-squares analysis, we found that the observed lines belong to four different splittings, which are resolved only when  $A \geq 1.0 \text{ mT}$ . It was impossible to find experimentally a crystal orientation where all the four splittings were simultaneously resolved. Only three out of four hyperfine tensors could be obtained with reasonable accuracy from the data analysis. Their principal values are listed in Table IV. The experimental errors are expected to be rather large (10%–20%), especially on the smallest hyperfine components. No indication could be found for the presence of more than four different couplings.

Since the  $D_{2d}$  symmetry lacks an inversion center, the eight selenium ligand atoms of the dodecahedron may give rise to eight magnetically inequivalent hyperfine splittings. Because

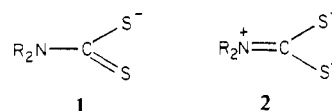
of the experimental results, we assume that four of these are definitely smaller than the others and are hidden under the main line width. With consideration of the natural abundance of  $^{77}\text{Se}$  (7.5%,  $I = 1/2$ ), the intensity of each satellite should be  $(0.075 \times 1/2)/0.70 = 5.4\%$  of the main peak, where 0.70 is the fraction of molecules which do not contain  $^{77}\text{Se}$  nuclei in any of the four "active" positions. Although in our spectra intensity measurements are complicated by the low resolution of the satellite lines, values close to the theoretical ones could be measured in some cases.

## Discussion

A comparison of the experimental results in Tables II and III with those already reported for analogous dithiocarbamato complexes<sup>1</sup> indicates a similar stereochemical arrangement. In both cases the effective ligand field experienced by the paramagnetic ions can be described as a strong  $D_{2d}$  perturbation with a superimposed small low-symmetry field, reducing the effective symmetry to  $D_2$  (B sites) or below (A sites).

The main difference between these two sets of data is in the absolute values of the magnetic parameters which indicate a markedly less covalent environment in the dithiocarbamato complexes.  $\text{V}/\text{Ti}(\text{Et}_2\text{dte})_4$ , A site, and  $\text{V}/\text{Mo}(\text{dta})_4$ , form I,<sup>1</sup> have close local symmetries (see below) so that differences in their magnetic parameters can be reasonably interpreted as a ligand effect. The  $g$  shifts from the free electron value are definitely larger in the former compound (ca. 10% for the  $g_z$  value), thus suggesting less covalent V–S bonds, lower contributions from the ligand spin-orbit coupling, and higher effective positive charge on the metal ion, i.e., higher effective metal spin-orbit coupling. The same trend is present in the metal hyperfine parameters, where the anisotropic terms  $|A_1 - A_{\text{av}}|$  which are expected to increase in the less covalent compound, raise from  $42.8 \times 10^{-4} \text{ cm}^{-1}$  in the dta complex to  $54.2 \times 10^{-4} \text{ cm}^{-1}$  in the dte complex. A similar behavior can be found in the related niobium complexes.

These effects are in line with "chemical intuition" and can be simply interpreted as due to the presence of the N atom allowing resonance structures of type 2, which give rise to an



effective dianionic electronic structure creating a larger ligand field. As a consequence dithiocarbamates behave as "harder" ligands than dithiocarboxylates, forming appreciably less covalent compounds. From this point of view the complexing properties of the dithiocarboxylato ligands resemble those of some recently reported dithiocarbamates,<sup>17,18</sup> for which aromatic effects make type 2 structures less favorable.

If we assume a  $D_2$  symmetry the ground-state function of a  $d^1$  system can be written as eq 1 with  $a^2 + b^2 = 1$ , where the coefficients  $a$  and  $b$  can be derived from the procedure described previously.<sup>1</sup>

$$\varphi_g = a|x^2 - y^2\rangle - b|z^2\rangle \quad (1)$$

Although the symmetry of the A sites is definitely lower than  $D_2$ , this choice allows the main low-symmetry effect, namely, configuration interaction among states belonging to the same irreducible representation, to be accounted for. No ligand orbitals have been included. The effects of covalency will be discussed on the basis of the modified spin-orbit and  $\langle r^{-3} \rangle$  parameters, or, more directly, on the basis of the selenium hyperfine couplings.

(16) Bradley, D. C.; Moss, R. H.; Sales, K. D. *J. Chem. Soc., Chem. Commun.* **1969**, 1255.

(17) Bereman, R. D.; Nalewajek, D. *Inorg. Chem.* **1977**, *16*, 2687.

(18) Bereman, R. D.; Nalewajek, D. *Inorg. Chem.* **1978**, *17*, 1085.

Table V. Best-Fit Parameters from the Analysis of the Metal Hyperfine Tensors<sup>a</sup>

compd	<i>a</i>	<i>b</i>	<i>b</i> <sup>2</sup> / <i>b</i> <sub>SAP</sub>	<i>P</i>	<i>K</i>
Nb/Ti(Et <sub>2</sub> dtc) <sub>4</sub> , site A	0.9894	0.145	8.4	111.4	113.2
V/Ti(Et <sub>2</sub> dtc) <sub>4</sub> , site A	0.9922	0.125	6.3	93.5	64.0
V/Ti(Et <sub>2</sub> dsec) <sub>4</sub> , site A	0.9915	0.130	6.8	85.4	65.8
Nb/Ti(Et <sub>2</sub> dsec) <sub>4</sub> , site B	0.9995	0.031	0.4	89.4	110.5
V/Ti(Et <sub>2</sub> dsec) <sub>4</sub> , site B	0.9995	0.030	0.4	76.5	65.6

<sup>a</sup> *P* and *K* are in units of 10<sup>-4</sup> cm<sup>-1</sup>. The limiting *a* and *b* values are, respectively, *a*<sub>Dod</sub> = 1, *b*<sub>Dod</sub> = 0, *a*<sub>SAP</sub> = 3<sup>1/2</sup>/2, *b*<sub>SAP</sub> = 1/2.

The results of the calculation are listed in Table V. They indicate a ground-state orbital of A symmetry mainly composed of  $|x^2 - y^2\rangle$  with some amount of  $|z^2\rangle$ . The  $|z^2\rangle$  admixture is almost the same for corresponding sites of the dithio- and diselenocarbamate complexes, thus confirming that the two host compounds have close molecular geometries. The  $b^2/b_{SAP}^2$  ratios indicate that the  $|z^2\rangle$  mixing ranges from 0.5 to 8% of that required by an ideal antiprismatic structure.

In this and in the preceding parts of this work, we have observed that the role of contributions different from the ligand-ligand repulsive energy and from the crystal packing forces in determining the molecular geometry of eight-coordinated complexes is difficult to assess experimentally. However the mixed-crystal compounds dealt with in this paper give some evidence for the presence of such effects. The pure compounds and Ti(Et<sub>2</sub>dtc)<sub>4</sub>, A site, have been shown to have close geometries, whereas a more symmetrical environment is present in Ti(Et<sub>2</sub>dtc)<sub>4</sub>, B site. If the two main effects recalled above were the only ones to control the stereochemistry of these complexes, we would have expected the two inequivalent sites of Ti(Et<sub>2</sub>dtc)<sub>4</sub> to be evenly populated. The preference of the d<sup>1</sup> ions toward the A site may indicate the presence of other effects, and  $\pi$  bonding appears to be the most reasonable. Although dithiocarbamates possess both empty and filled  $\pi$  orbitals, their  $\pi$ -donor properties are certainly more pronounced than those of dithiocarboxylates, due to the greater donor character of the substituent on the CS<sub>2</sub><sup>-</sup> group. This means that the interaction of the half-filled  $|x^2 - y^2\rangle$  metal orbital with the filled  $\pi_{\perp}$  orbitals of the ligands is progressively more important. Since this interaction is a destabilizing one in pure *D*<sub>2d</sub> symmetry<sup>7</sup> and can be relieved only by some distortion, the preference of the d<sup>1</sup> ions toward the most asymmetric site of Ti(Et<sub>2</sub>dtc)<sub>4</sub> can be rationalized.

The calculated isotropic hyperfine terms,  $K = -g_e g_n \mu_b \mu_n \langle 2/3\chi \rangle$ , where  $\chi$  represents the polarization of the inner-shell *s* electrons,<sup>19</sup> are in reasonable agreement with the experimental *A*<sub>av</sub> values, the two quantities being related by the expression  $A_{av} = -K + (g_{av} - g_e)P$ . The best-fit *P* values, where *P* is the anisotropic hyperfine term  $g_e g_n \mu_b \mu_n \langle r^{-3} \rangle$ , are strongly reduced with respect to the free ion values but definitely larger than the *P* values calculated for corresponding dithiocarboxylato complexes, in agreement with the higher covalency of the latter. V/Ti(Et<sub>2</sub>dtc)<sub>4</sub>, A site, and V/Mo(dta)<sub>4</sub>, form I, give, respectively, 93.5 and 78.0 cm<sup>-1</sup>. Even in the case of V/Ti(Et<sub>2</sub>dsec)<sub>4</sub>, for which extensive delocalization of the unpaired electron is expected, the values reported are higher than or similar to those found for vanadium tetrakis(dithiocarboxylato) compounds.

Ligand hyperfine structure for eight-coordinated complexes has been previously observed only in the [Mo(CN)<sub>8</sub>]<sup>3-</sup> ion. This highly covalent compound gave a solution EPR spectrum with an isotropic <sup>13</sup>C hyperfine constant of 10.9 × 10<sup>-4</sup> cm<sup>-1</sup>.<sup>8</sup> However, no splitting could be detected in the powder spectrum of the same compound diluted in K<sub>4</sub>[Mo(CN)<sub>8</sub>]·2H<sub>2</sub>O.<sup>9</sup> Presumably this is due both to the lower intrinsic resolution

of powder spectra and to the symmetry change (*D*<sub>4d</sub> → *D*<sub>2d</sub>) that [Mo(CN)<sub>8</sub>]<sup>3-</sup> undergoes going from the solution to the solid state.

As already mentioned, the satellites flanking the main peaks of V/Ti(Et<sub>2</sub>dsec)<sub>4</sub> have been interpreted as <sup>77</sup>Se lines on the basis of two main facts: (i) their spacing and intensity are anisotropic but strictly field independent, as expected for a "true" hyperfine interaction; (ii) the experimental line intensity is close to the theoretical value for <sup>77</sup>Se in all the spectra for which reliable intensity measurements were possible.

An interesting outcome of the measured hyperfine splitting is the clear discrimination between the so-called A and B dodecahedral sites (Figure 1a).

The spin-density distribution between a magnetic ion and its surrounding ligands is the result of direct overlap and charge-transfer mechanisms, both effects being proportional to the overlap integral.<sup>20</sup> In *D*<sub>2d</sub> symmetry the metal ground-state orbital  $|x^2 - y^2\rangle$  is strictly  $\sigma$  nonbonding and any spin transfer must occur through a  $\pi$ -bonding mechanism ( $\pi_{\perp}$  orbital in the *mmmm* isomer). The overlap integral between  $|x^2 - y^2\rangle$  and a  $\pi_{\perp}$  orbital is  $S(\theta) = S_{\pi} \sin \theta$ , where  $\theta$  is the angle between the metal-ligand bond direction and the  $\bar{4}$  axis and  $S_{\pi}$  is the limiting value of the integral.<sup>7</sup> The  $\theta$  values for the A and B ligands in Ti(Et<sub>2</sub>dtc)<sub>4</sub>, molecule 1, are 35.4 and 77.0°, respectively. Since  $A^{Se}$  is roughly proportional to  $S^2(\theta)$ , the maximum value of  $A^{Se}$  is expected to be around  $7 \times 10^{-4}$  cm<sup>-1</sup> from a  $S_A^2(\theta)/S_B^2(\theta)$  value of 2.8. The estimated upper limit for  $A^{Se}$  is well below the spectral resolution and accounts for the experimental observation of only four selenium splittings.

The three selenium hyperfine tensors which could be refined are almost equivalent, as expected for an essentially Dod symmetry. Their isotropic and anisotropic components have an average value of 14.3 and  $4.8 \times 10^{-4}$  cm<sup>-1</sup>. From these values the coefficients of the selenium 4s and 4p orbitals in the MO of the unpaired electron can be obtained from expressions 2 and 3 and the reported values of  $|\psi_{4s}(0)|^2$  and  $\langle r^{-3} \rangle_{4p}$ .<sup>21</sup>

$$A_{av}^{Se} = \frac{8}{3} \pi g_e g_n \mu_b \mu_n |\psi_{4s}(0)|^2 c_{4s}^2 \quad (2)$$

$$A_{Se_1} - A_{av}^{Se} = \frac{4}{5} g_e g_n \mu_b \mu_n \langle r^{-3} \rangle_{4p} c_{4p}^2 \quad (3)$$

The calculated coefficients are  $c_{4p} = 0.190$  and  $c_{4s} = 0.173$  with  $c_{4p}^2/c_{4s}^2 = 1.2$ . This means that about 7% of the total unpaired spin density is transferred on each Se<sub>A</sub> ligand, in an orbital composed of 4s and 4p in roughly the same amount.

Finally, the principal *g* values and orientations of V/Ti-(Et<sub>2</sub>dsec)<sub>4</sub> require some further comment. Their deviations from the free electron value are small or zero, whereas negative *g* shifts are predicted in all cases from conventional ligand-field expressions. Moreover, the *g* tensor eigenvectors are unique among all the eight-coordinated complexes investigated in that the lowest *g* value is almost perpendicular to the molecular *z* axis instead of being parallel to it.

Similar effects are not new and have been found in several other complexes containing selenium<sup>22,23</sup> or any other heavy ligand atoms.<sup>24</sup> They have been shown to be the result of large ligand spin-orbit coupling constants and low-energy ligand d

(20) Simanek, E.; Stroubek, Z. In "Electron Paramagnetic Resonance"; Geschwind, S., Ed.; Plenum Press: New York, 1972.

(21) Wertz, J. E.; Bolton, J. R. "Electron Spin Resonance"; McGraw-Hill: New York, 1972.

(22) Keijzers, C. P.; Paulussen, G. F. M.; de Boer, E. *Mol. Phys.* **1975**, *29*, 973.

(23) Attanasio, D.; Keijzers, C. P.; van de Berg, J. P.; de Boer, E. *Mol. Phys.* **1976**, *31*, 501.

(24) Barbucci, R.; Bencini, A.; Gatteschi, D. *Inorg. Chem.* **1977**, *16*, 2117.

(25) Hoard, J. L.; Silverton, J. V. *Inorg. Chem.* **1963**, *2*, 235.

functions, which give sizeable contributions to the  $g$  value expressions in a strongly covalent system. In this case bonding parameters are difficult to extract from the  $g$  values, and they can be interpreted and reproduced only on the basis of a

complete molecular orbital calculation.

Registry No. Nb(Et<sub>2</sub>dte)<sub>4</sub>, 12406-69-8; Ti(Et<sub>2</sub>dte)<sub>4</sub>, 12367-51-0; Ti(Et<sub>2</sub>dsec)<sub>4</sub>, 80340-09-6; V(Et<sub>2</sub>dte)<sub>4</sub>, 12406-70-1; V(Et<sub>2</sub>dsec)<sub>4</sub>, 80340-10-9.

Contribution from the Department of Chemistry,  
University of South Carolina, Columbia, South Carolina 29208

## Spectra and Structure of Gallium Compounds. 4.<sup>1a</sup> Vibrational Studies of Ammonia-Trimethylgallane and Ammonia-*d*<sub>3</sub>-Trimethylgallane

J. R. DURIG,\* C. B. BRADLEY,<sup>1b</sup> and J. D. ODOM

Received October 21, 1981

The infrared (80–4000 cm<sup>-1</sup>) and Raman (25–3500 cm<sup>-1</sup>) spectra of (CH<sub>3</sub>)<sub>3</sub>Ga·NH<sub>3</sub> and (CH<sub>3</sub>)<sub>3</sub>Ga·ND<sub>3</sub> have been recorded for the solid state at 77 K. The spectra have been interpreted on the basis of C<sub>3v</sub> molecular symmetry. None of the A<sub>2</sub> vibrations have been observed although a lower site symmetry in the solid state is indicated by the splitting of the bands assigned to the NH<sub>3</sub> and GaC<sub>3</sub> antisymmetric stretching modes. Additionally many of the symmetric modes (A<sub>1</sub>) are split into two bands by the crystal field which indicates at least two molecules per primitive unit cell. The valence force field model has been utilized in calculating the frequencies and the potential energy distribution. The calculated potential constants for the adducts are compared to those previously reported for the Lewis acid and base moieties, and the differences are shown to be consistent with structural changes upon adduct formation. Only very minor coupling has been observed between the Ga–N stretch and several of the GaC<sub>3</sub> modes. The Ga–N force constant has been found to have a value of 1.08 mdyn/Å, which is much smaller than the value of the Ga–N force constant (2.43 mdyn/Å) in (CH<sub>3</sub>)<sub>3</sub>N·GaH<sub>3</sub>. The magnitudes of these force constants appear to adequately reflect the relative stabilities of the adducts.

### Introduction

The relative donor strengths of nitrogen- and phosphorus-containing compounds toward a given acceptor have been a subject of continuing interest in coordination chemistry. We have recently studied<sup>2,3</sup> the spectra and structure of three coordination compounds of gallium: (CH<sub>3</sub>)<sub>3</sub>P·GaH<sub>3</sub>, (C-H<sub>3</sub>)<sub>3</sub>N·GaH<sub>3</sub>, and (CH<sub>3</sub>)<sub>3</sub>Ga·PH<sub>3</sub>. In our studies of the first and second compounds we found that the Ga–P stretching force constant has a value of 2.0 mdyn/Å, which is much smaller than the value of the Ga–N force constant (2.43 mdyn/Å) in (CH<sub>3</sub>)<sub>3</sub>N·GaH<sub>3</sub>; however, this does not reflect the relative stabilities of these adducts as determined by other methods.<sup>4</sup> In an NMR study, Leib et al.<sup>5</sup> reported that the ammonia adduct of trimethylgallane was more stable than the corresponding adduct formed with trimethylphosphine but less stable than the adduct formed with trimethylamine. However, these authors<sup>5</sup> did not investigate the relative stability of the (CH<sub>3</sub>)<sub>3</sub>Ga·PH<sub>3</sub> adduct since it has only recently been prepared.<sup>3</sup> In our investigation of (CH<sub>3</sub>)<sub>3</sub>Ga·PH<sub>3</sub> we found this molecule to be relatively unstable at ambient temperature with the evolution of a noncondensable gas which is similar to the thermal decomposition of ammonia-trimethylgallane where a dimeric derivative containing three-center bonds is generated.<sup>6</sup>

Recently, we<sup>2b</sup> studied the microwave spectrum of (C-H<sub>3</sub>)<sub>3</sub>N·GaH<sub>3</sub> and obtained an  $r_s$  distance of 2.111 ± 0.002 Å for the Ga–N bond. This distance is considerably shorter than the Ga–N bond distance of 2.20 Å reported<sup>7</sup> for the (C-H<sub>3</sub>)<sub>3</sub>Ga·N(CH<sub>3</sub>)<sub>3</sub> molecule. Since (CH<sub>3</sub>)<sub>3</sub>Ga·NH<sub>3</sub> is isomeric

with trimethylamine-gallane, we have investigated the low-temperature infrared and Raman spectra of ammonia-trimethylgallane in order to examine possible differences in the molecular structures of the two isomers and to determine the acid-base strengths of the donors and the acceptors involved in the Ga–N bonding. Additionally, it was hoped that we could obtain a microwave spectrum of (CH<sub>3</sub>)<sub>3</sub>Ga·NH<sub>3</sub> from which the Ga–N bond distance could be ascertained. The results of these investigations are reported herein.

### Experimental Section

The samples of (CH<sub>3</sub>)<sub>3</sub>Ga·NH<sub>3</sub> and (CH<sub>3</sub>)<sub>3</sub>Ga·ND<sub>3</sub> were prepared and handled with standard high-vacuum techniques in a system equipped with greaseless stopcocks. The synthesis was carried out in a Pyrex tube fitted with a greaseless stopcock by condensing into the tube approximately equimolar amounts of (CH<sub>3</sub>)<sub>3</sub>Ga, purchased from Alfa (electronic grade, 99.9+% pure) and used without further purification, and NH<sub>3</sub> or ND<sub>3</sub>, prepared according to the literature<sup>8</sup> and purified by passage through two –78 °C traps into a –196 °C trap. The (CH<sub>3</sub>)<sub>3</sub>Ga was used in slight excess to minimize multiple coordination. The reactants were allowed to warm to room temperature, the compound forming quickly as a clear-white semicrystalline solid. The tube was then cooled to –45 °C and the excess (CH<sub>3</sub>)<sub>3</sub>Ga pumped out.

The Raman spectra (Figure 1) were recorded from 25 to 3500 cm<sup>-1</sup> on a Cary Model 82 laser Raman spectrophotometer using a Spectra Physics Model 171 argon ion laser tuned to the 514.5-nm line at the excitation source. The amount of power measured at the sample was typically 1 W. Frequencies of the peaks were measured with a spectral band width of 2 or 3 cm<sup>-1</sup>. The monochromator was calibrated against mercury emission lines, and frequencies for sharp resolvable lines are expected to be accurate to ±2 cm<sup>-1</sup>. The sample was slowly deposited onto a blackened brass block, held at an angle of 75° from the normal and cooled by boiling liquid nitrogen, and annealed until no further change was observed in the spectrum.

The mid-infrared spectra from 200 to 4000 cm<sup>-1</sup> (Figure 2) were recorded on a Perkin-Elmer Model 621 grating infrared spectrophotometer. The housing was purged with dry nitrogen, and the instrument was calibrated with standard gases in the high-frequency region and with water vapor in the low-frequency region. Sharp resolvable bands are expected to be measured accurately to ±2 cm<sup>-1</sup>. The sample was condensed onto a cesium iodide substrate mounted

- (1) (a) For part 3, see *J. Mol. Struct.* **1981**, *72*, 73. (b) Taken in part from the thesis of C. B. Bradley which will be submitted to the Department of Chemistry in partial fulfillment of the Ph.D. degree.
- (2) (a) Odom, J. D.; Chatterjee, K. K.; Durig, J. R. *J. Phys. Chem.* **1980**, *84*, 1843. (b) Durig, J. R.; Chatterjee, K. K.; Li, Y. S.; Zozulin, A. J.; Odom, J. D. *J. Chem. Phys.* **1980**, *73*, 21.
- (3) Odom, J. D.; Chatterjee, K. K.; Durig, J. R. *J. Mol. Struct.* **1981**, *72*, 73.
- (4) Greenwood, N. N.; Ross, E. J. F.; Storr, A. J. *Chem. Soc.* **1965**, 1400.
- (5) Leib, A.; Emerson, M. T.; Oliver, J. P. *Inorg. Chem.* **1965**, *4*, 1825.
- (6) Durrant, P. J.; Durrant, B. "Introduction to Advanced Inorganic Chemistry", 2nd ed.; Wiley: New York, 1970; p 584.
- (7) Golubinskaya, L. M.; Golubinskii, A. V.; Mastryukov, V. S.; Vilkov, L. L.; Bregadze, V. I. *J. Organomet. Chem.*, **1976**, *117*, C4.

- (8) Herber, R. H., Ed. "Inorganic Isotopic Syntheses"; W. A. Benjamin: New York, 1962.